Oceanologia (2020) 62, 443—459

Available online at www.sciencedirect.com

ScienceDirect

journal homepage: www.journals.elsevier.com/oceanologia

ORIGINAL RESEARCH ARTICLE

Tidal characteristics in the Gulf of Khambhat, northern Arabian Sea — based on observation and global tidal model data

Aditi Mitra[a,b], **V. Sanil Kumar**[a,*], **Basanta K. Jena**[c]

[a] *Ocean Engineering, CSIR-National Institute of Oceanography (Council of Scientific and Industrial Research), Dona Paula, Goa, India*
[b] *Research Scholar, Bharathidasan University, Tiruchirappalli,Tamil Nadu, India*
[c] *Coastal and Environmental Engineering Division, National Institute of Ocean Technology, Pallikaranai, Chennai, India*

Received 4 September 2019; accepted 28 May 2020
Available online 7 June 2020

KEYWORDS
Gulf of Khambhat;
Semi-enclosed basins;
Tidal constituents;
Tidal propagation;
Sea-level

Summary Tidal characteristics of the Gulf of Khambhat are described based on measured and modelled sea-level data. Data were recorded at three locations inside and two locations outside the Gulf with record lengths of 6—12 months to study the tidal propagation. A northward increase in tidal amplitude is noticed from Daman (eastern side) and Diu (western side) and attains maxima at Bhavnagar. A similar trend is followed by the amplitude of the major tidal constituents, although there are discrepancies for that of the minor constituents. The non-tidal factor which influences the sea-level is the local wind, especially the alongshore component of wind. A positive correlation is obtained between the sea-level and the meridional component of wind at each location. Harmonic analysis of sea-level data shows that M2 is the major tidal constituent which propagates in a non-linear fashion inside the Gulf. Tides from two global tide models (MIKE21 and FES2014) have been compared with the measured data, which could be used for further prediction of the tides and sediment transport in the Gulf. The tide elevation derived from the MIKE21 model has further been used for the harmonic analysis of tide. The tides predicted using one-month data are up to 10% smaller than those predicted using the one-year data. The global tide model FES2014 data performs well with measured data for offshore

* Corresponding author at: Ocean Engineering, CSIR-National Institute of Oceanography (Council of Scientific and Industrial Research), Dona Paula, Goa-403 004, India. Tel.: +91 832 2450 327.
E-mail address: sanil@nio.org (V.S. Kumar).
Peer review under the responsibility of the Institute of Oceanology of the Polish Academy of Sciences.

Production and hosting by Elsevier

https://doi.org/10.1016/j.oceano.2020.05.002

locations, whereas it fails to predict the same for the inner Gulf locations. The study manifests the fact that to understand the dynamics of complex tidal areas, regional models should better be used than global tidal models.

1. Introduction

Information on tides along a coastline is vital for estimating the top level of the coastal protection structures and port structures. Ocean tides have long been thought of as a stationary process as they are driven by the gravitational forcing of Sun and Moon, whose motions are complex but highly predictable (Cartwright and Taylor, 1971). Tidal propagations in estuaries are affected by freshwater discharge and friction (Dronkers, 1964), besides changes in depths and the morphology of the channel (Carl and Aubrey, 1994; Dronkers, 1964; Godin, 1993; Lanzoni and Seminara, 1998; Shetye and Gouveia, 1998), which implies variations in the mean water level and asymmetry of the tidal wave. Tidal asymmetry in a shallow-water system could be explained through the generation of overtides and compound tides (Dronkers, 1964; Pugh, 1987). The shallow water tides contribute to differences between Mean Tide Level and Mean Sea-Level (MSL) (Woodworth, 2017); tides can also exhibit short-term variability correlated to short-term fluctuations in MSL (Devlin et al., 2014; 2017a, b). The astronomical tide is strongly distorted during its propagation from offshore into the shallow inlet/estuarine systems. This distortion could be represented as the non-linear growth of harmonics of the principal ocean astronomical constituents (Aubrey, 1985).

Measured sea-level data comprises contributions from mean sea-level, astronomical tides, vertical land movements, meteorologically and oceanographically induced water level changes and episodic water level fluctuations due to climate extremes, systematic bias and noise. The analysis of correlations between tides and sea-levels at a local or regional scale can indicate locations where tidal evolution should be considered a substantial complement to sea-level rise (Devlin et al., 2019). Removal of the tidal component from the sea-level data leaves residuals of sea-level that include contributions from atmospheric components and surface waves (Kumar et al., 2011). In the estuaries and river mouth, the river discharge also contributes to the residual component. Residual sea-level also results from the friction of the system. The combined influence of the tidal phase, amplitude and spatial gradient in MSL on the generation of the residuals of sea-level in a channel is complex and non-linear and could be predicted properly only by a non-linear numerical model (Liu and Aubrey, 1993). Unnikrishnan et al. (1999) used a barotropic numerical model based on shallow water wave equations to simulate the sea-level and circulation in the Gulf of Khambhat and surrounding areas. Sea-level variations due to surges triggered by storm winds form a noise superimposed on the highly periodic tides, which have an astronomical origin (Sundar et al., 2005). The generation of residuals of sea-level in a tidal channel is the most sensitive to the spatial gradient in MSL, less sensitive to the tidal amplitude difference and least sensitive to the tidal-phase difference. It directly influences material transport, i.e., suspended sediment, pollutants, etc. in a shallow channel. The study based on simultaneously measured sea-level data at three locations covering a distance of 100 km along the west coast of India indicates that the variations in sea-level due to tide is ~96% (Kumar et al., 2011). An understanding of the seasonal cycle of sea-level forms an important component of climate studies. It has some practical implications as well, e.g., the accurate tidal prediction tables for a coastline (Wijeratne et al., 2008).

The Gulf of Khambhat (GoK, hereafter referred to as the Gulf) is one of the highly energetic macro-tidal regimes of the north-eastern Arabian Sea and the other area in the north-eastern Arabian Sea is the Gulf of Kutch (Shetye, 1999). Although there are quality studies carried out in the Gulf from the past two decades or more, the area lags in long-term in situ datasets on hydrodynamic parameters. The previous studies mainly focused on modelled data to obtain the hydrodynamics of the Gulf. The present study utilises measured sea-level data at different locations to discern the tidal propagation in the Gulf. The observed tides have been compared with the data derived from the global tide models (MIKE21 and FES2014) to examine the behaviour of the global model at a regional scale. The study also focuses on ascertaining the major astronomical tidal constituents, which contribute to the tidal amplitude. The present study puts up an effort to determine the tidal and non-tidal components of the sea-level of the Gulf, based on numerical experiments. Even though the amplification inside the Gulf is a well-known phenomenon, a contemporary approach has been adopted in the present study. As the tidal phenomena of the Gulf are more complex than any other coastal waters of India, it is important to assess the global models to reveal their strengths and weaknesses in terms of their performances.

2. Study region

The GoK (formerly known as the Gulf of Cambay) is a funnel-shaped indentation situated between the Saurashtra peninsula and the mainland of Gujarat (Fig. 1). The western continental shelf of India varies from south to north, widens off Mumbai and leads into a strongly converging channel, the GoK. The GoK has a width of 80 km at the mouth and funnels down to 25 km over the longitudinal reach of 140 km. The Gulf has acquired significance because of its geographic proximity to two industrially important states viz. Gujarat and Maharashtra as it provides an easy opening to sea for transportation of materials to several industries around it. The tides in GoK are of a semi-diurnal type with a large diur-

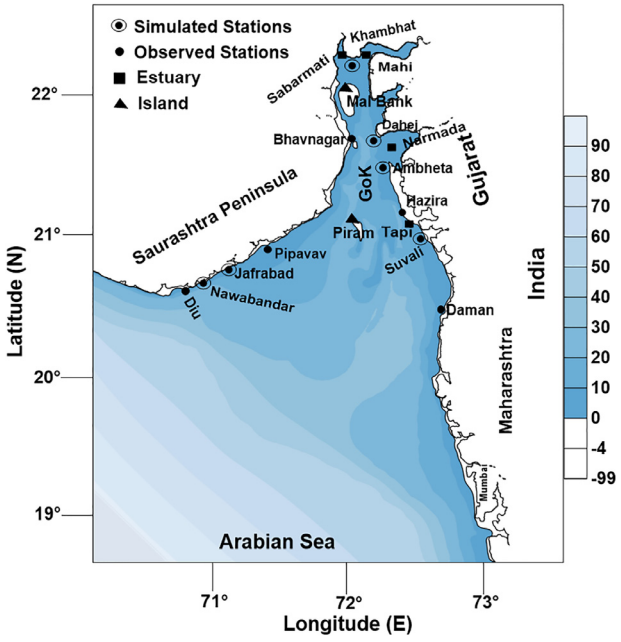

Figure 1 Study area with bathymetry of the region. The sea-level measurement locations are also shown in the figure.

nal inequality and varying amplitudes, which amplifies from the south to north along the GoK in the continental shelf and in the main Gulf (except Gulf head regions). This important characteristic of the embayment results from the quarter wavelength resonance of the tides owing to its inherent geometrical settings (Nayak and Shetye, 2003). In GoK, the tidal front experiences phase-shift due to geometric effects caused by shallow inner regions, narrowing cross-sections and uneven bottom topography. Tide gets amplified significantly inside the Gulf due to its shape and varying bottom friction coefficients (Nayak and Shetye, 2003) and the large width of the continental shelf off the north-western coast of India (Joseph et al., 2009). In the northern Arabian Sea, the maximum tidal range is found in GoK with an average tidal range of 10 m near to Bhavnagar (Kumar et al., 2006). Semi-diurnal tides in the GoK, amplify about threefold from mouth to head; in contrast, the amplification of diurnal tides is much smaller (Nayak and Shetye, 2003). It is reported that currents in the Gulf are predominantly tide-induced with speed up to 3.3 m/s and the currents are north-northwest during flood tide and south-southeast during ebb tide (Kumar and Kumar, 2010).

3. Material and methods

Time-series data of sea-level recorded with tide gauges at three locations inside and two locations outside the Gulf are used in the study. The locations and sampling periods of sea-level and wind-speed are presented in Table 1. Data were missed in a few locations for short periods due to the failure of the instrument. The observed datasets remained discontinuous (wherever used as model inputs) to avoid computational errors due to the missing datasets. The sea-level data is subjected to the standard harmonic analysis by fitting a finite set of cosine functions having frequencies at the known astronomical forcing frequencies by the least square method. Tidal Analysis Software Kit (TASK) (Bell et al., 2000) developed by the Proudman Oceanographic Laboratory, UK, is used for the harmonic analysis and to separate the tidal and residual components from the measured sea-level data. The harmonic analysis is performed using 24 major (Q1, O1, M1, K1, J1, OO1, M2, N2, L2, S2, 2SM2, MU2, MO3, M3, MK3, MN4, M4, MS4, SN4, 2MN6, M6, MSf, 2MS6 and 2SM6) and eight related (PI1, PSI1, P1, PHI1, 2N2, T2, NU2 and K2) tidal constituents in the analysis of six and twelve-monthly records. Based on their amplitude, only major 13 tidal constituents (M2, S2, K1, N2, O1, K2, P1, MU2, M4, MS4, NU2, L2 and MSf) are used in this study. The time and the phase lag reported in the paper is the local time, which is 5 hours 30 minutes ahead of the Greenwich Mean Time (GMT). Residual sea-levels are also estimated for a period of one year in Daman, Hazira and Bhavnagar and for six months in Pipavav and Diu with the help of TASK. Monthly MSL is obtained by calculating the monthly average sea-level for each month at each station. Sea-Level Anomaly (SLA) is determined by the following formula (Eq. 1):

$$SLA = \frac{1}{n}\sum_{i=1}^{n}(T_{e_i} - T_m), \quad (1)$$

where, T_e – tide elevation, T_m – mean tide.

Reanalysis data of meridional and zonal components of wind at 10 m height at 6 hourly intervals from NCEP/NCAR (Kalnay et al., 1996) is obtained for the study area corresponding to the tide gauge record period to know the influence of wind on sea-level. These data are provided by the NOAA-CIRES Climate Diagnostics Centre, Boulder, Colorado, at http://www.cdc.noaa.gov/.

The tides estimated based on the tidal constituents available with the MIKE21 Global Tide Model (DHI, 2017) at six locations covering the Gulf is also used to determine the tidal propagation inside the Gulf. The Global Tide Model is developed by DTU Space (DTU10) and is available on a 0.125 × 0.125-degree resolution grid for the major 10 constituents in the tidal spectra. The model is utilizing the latest 17 years' multi-mission measurements from TOPEX/Poseidon (Phase A and B), Jason-1 (Phase A and B) and Jason-2 satellite altimetry for sea-level residual analysis. Based on these measurements, harmonic constituents have been calculated.

Global Finite Element Solution (FES2014) (Carrere et al., 2015), which is the latest version of the FES series, is utilized to obtain the tide data at the locations where in situ data is recorded. It usually shows higher accuracy in shallow water zones because of finer bathymetry and an optimized assimilation scheme (Seifi et al., 2019). The distances of all the locations referred in the study from the Gulf mouth are presented in Table 2.

4. Results

4.1. Tide elevation

Daman is chosen as a location outside the Gulf mouth in the eastern GoK, where sea-level variation is measured for a period of one year (Fig. 2a). Maximum spring and neap tidal

Table 1 Measurement locations and period of recording of sea-level and wind.

Locations	Latitude/Longitude	Period of recording	Highest sea level measured (m)	Mean sea level from measured data (m)	Mean sea level from hydrographic chart from chart datum (m)
Daman	20.4124°N 72.8319°E	01.01.2014— 31.12.2014	6.32	2.88	3.80
Hazira	21.0860°N 72.6233°E	01.01.2014— 31.12.2014	8.42	4.19	4.50
Bhavnagar	21.8427°N 72.2562°E	01.01.2014— 31.12.2014	11.66	5.82	6.10
Pipavav	20.9163°N 71.5066°E	01.01.2014— 24.06.2014	4.85	2.47	1.80
Diu	20.7192°N 70.9952°E	01.01.2014— 31.05.2014	2.80	1.71	1.50

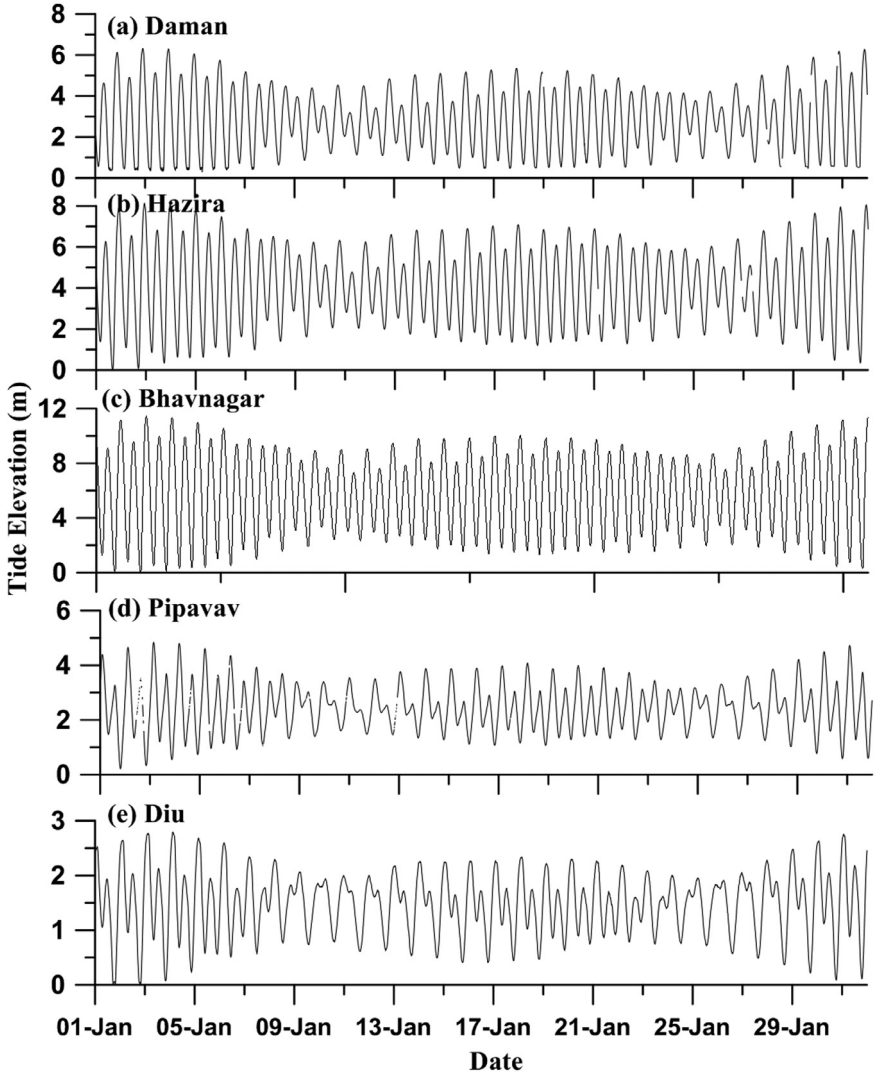

Figure 2 Time series plot of the measured tide data from 1 January to 31 January 2014 at a) Daman, b) Hazira, c) Bhavnagar, d) Pipapvav and e) Diu. Tides are presented with respect to Chart Datum.

Table 2 Locations and their distance from mouth of GoK where positive, negative and zero denotes inside, outside and Gulf mouth respectively.

Locations	Distance from Gulf mouth (km)
Daman	-51.3
Suvali	0
Ambheta	38
Hazira	55
Dahej	106
Khambhat	156.3
Bhavnagar	127
Pipavav	0
Jafrabad	-25
Nawabandar	-58
Diu	-73

elevations at Daman are 6.5 m and 5.5 m, respectively. At this location, data could not be collected continuously for one-year due to instrumental error. Hazira, a location inside GoK, is selected from the eastern coast, where observations on sea-level are taken for one year. Neap-spring variation at Hazira ranged between 7 and 8.1 m, respectively (Fig. 2b). Bhavnagar is selected inside the GoK in the western coast, where the tidal range is found to be maximum among all the locations. The maximum spring tidal height is found to be 11.6 m and the maximum neap tidal height is 10 m (Fig. 2c). Data is missed for a couple of short periods in this location due to instrumental error. Another location, selected from the western coast situated at the Gulf mouth is Pipavav, where the tide elevation is comparatively low. In situ data of sea-level is recorded for six months at Pipavav. Neap and spring tide elevations are 4 and 4.8 m, respectively, on an average (Fig. 2d). Diu is chosen outside GoK at the Saurashtra coast, where tide elevation is recorded for six months. The neap and spring variation is 2 and 2.8 m, respectively (Fig. 2e). Minimum variation in sea-level is noticed at Diu among all the five locations. Analysis of one-year-long sea-level data for three locations and six-months-long data for two locations indicates that GoK is a non-linear shallow-water system.

4.2. Comparison of model output with the measured tide

4.2.1. MIKE21 Global Tide Model

Tide elevation data are derived with the help of the MIKE21 Global Tide Model at the locations of observed data. The elevations are well-in agreement at all the locations except Hazira, where a discrete difference between modelled and the observed tide has been noticed (Fig. 3). The statistical parameters calculated based on the observed data sets and MIKE21- derived datasets are presented in Table 3. Overall, both these datasets are well in agreement with each other. Thus, this model is further used to predict tide elevations at several other locations of the Gulf.

4.2.2. FES2014 Global Tide Model

Tide elevation data are extracted from the global tidal model FES2014 for the same period of time for the locations where in situ data of tide elevation are recorded. A comparison is made between the measured and FES2014 data (Fig. 4). A good match is obtained between the measured and FES2014 data at the offshore stations, i.e., Daman and Diu. A good match could be seen even at the inner station of Pipavav. If we proceed further inside the Gulf, i.e., at Hazira and Bhavnagar, the FES2014 and measured data are not in agreement with each other. For both these locations, FES2014 data underestimated the measured tide level. The amplitudes of the major semi-diurnal and diurnal tidal constituents estimated from FES2014 are similar to the values obtained from measured data for the offshore locations, whereas, for locations like Hazira and Bhavnagar, the amplitudes of the constituents differ (Table 4).

4.3. Harmonic analysis

4.3.1. Amplitude

The major tidal constituents evaluated in the present study are grouped as diurnal (K1, O1, P1), semi-diurnal (M2. S2, N2, K2, L2) and mixed (MU2, M4, MS4, NU2, MSf). Out of the 13 major astronomical constituents used in the study based on their amplitude, five diurnal and semi-diurnal constituents are represented together in Fig. 5a. Similarly, a total of eight diurnal, semi-diurnal, compound and overtide constituents are presented together in Fig. 5b. The dominant tidal constituent is M2, with the amplitude four times greater than the major diurnal or semi-diurnal constituents. The increase in amplitude is found to be more regular from Gulf mouth to head in case of the eastern coast, while irregularity in the amplification is observed in the western coast. From Daman to Hazira, M2 has propagated a distance of 85 km, with an increase of 0.443 m (rate of 0.005 m per km). The rate increased to 0.014 m per km while moving from Hazira to Bhavnagar, covering a distance of 117 km. Minimum amplitude is noticed outside GoK at Diu (~0.48 m). The maximum amplitude is at Bhavnagar (3.33 m), which has a dramatic decrease at Pipavav with a rate of 0.02 m per km. There is a gradual increase in amplitude from Gulf mouth to head along both the coasts of GoK for the other major constituents.

Even in the case of the minor constituents, an irregular increase from Gulf mouth to head is observed. In this case, the maximum amplitude is noticed for K2, with an amplitude two times higher than the other minor constituents on an average. MSf tide is taken into consideration as this is the largest among the fortnightly constituents. It consists of both an elementary component, which is part of the equilibrium tide and a possible forced component arising from the interaction of M2 and S2 (S2-M2). It did not have a consistent trend of variation in the study region with a maximum of 0.048 m at Pipavav.

Propagation of major diurnal and semi-diurnal tide is studied with the help of tidal constituents available in the MIKE21 Global Tide Model at six locations throughout the Gulf. The trend is similar to the in situ measurements (Fig. 6a). M2 is the most dominant constituent in each of the locations. It had an amplitude of 2.057 m at Suvali, which got increased to 2.708 m at Ambheta. A sudden decrease is obtained at Dahej (1.623 m), which again increased northward at Khambhat. A similar trend of increase is obtained along the western coast towards the north and with mini-

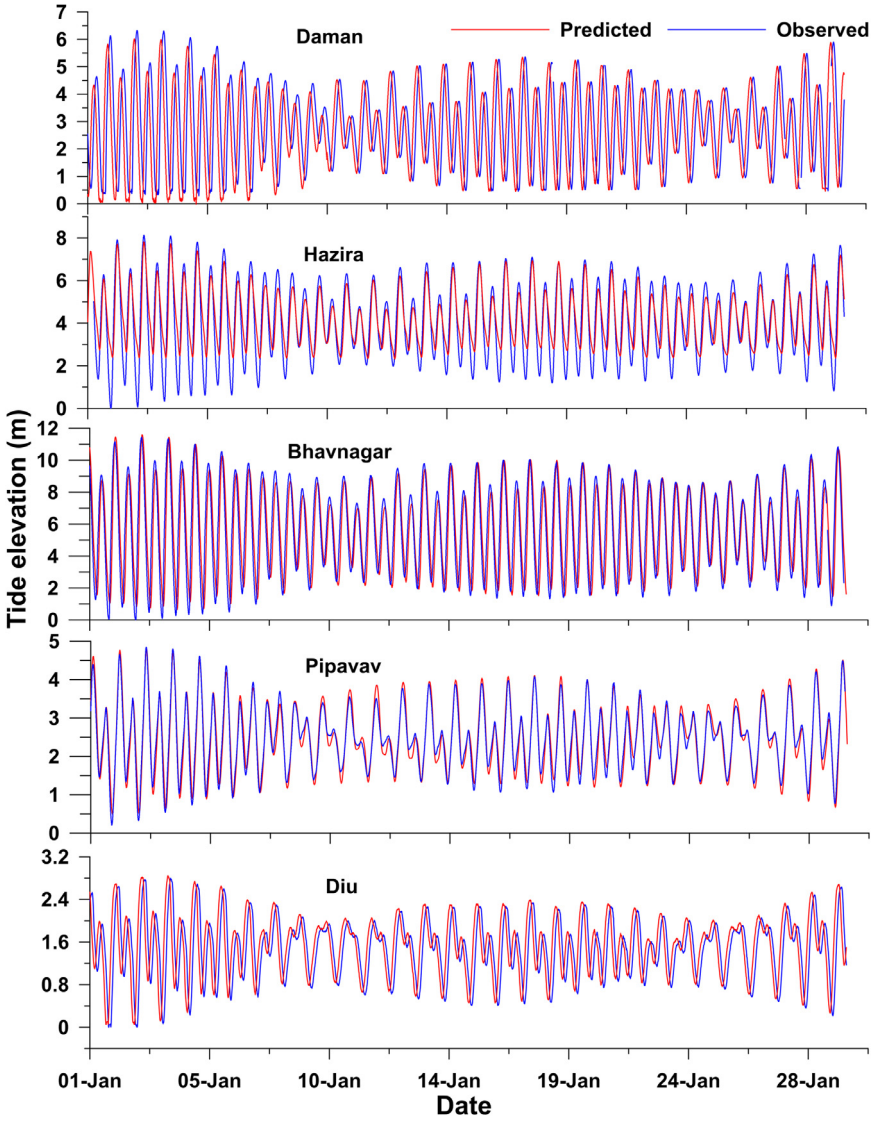

Figure 3 Comparison between predicted tide based on MIKE21 Global Tide Model and observed tide at Daman, Hazira, Bhavnagar, Pipapvav and Diu.

Table 3 Correlation (r), bias, Root Mean Square Error (RMSE) and significance level (p-value) between 2D model derived tide and observed tide in Daman and Pipavav, correlation between v-component of wind and tide residual.

Statistical Parameters	Predicted (MIKE21) and observed tide					v-component of wind and tide residual				
	Daman	Hazira	Bhavnagar	Pipavav	Diu	Daman	Hazira	Bhavnagar	Pipavav	Diu
r	0.8	0.45	0.78	0.73	0.76	0.33	0.22	0.04	0.06	0.17
Bias (m)	-0.03	-0.02	-0.04	-0.02	0.02	-	-	-	-	-
RMSE (m)	0.02	0.04	0.03	0.01	0.03	-	-	-	-	-
p-value	0.04	0.02	0.04	0.03	0.02	-	-	-	-	-

mum magnitude at Nawabandar. S2 tide had a gradual increase towards the north along both the coasts of GoK. The O1 tide follows a similar trend of propagation. There is no regularity of variation in the case of K1.

Influences of the length of the dataset and period of the data on the evaluation of the tidal constituents are studied by considering one-month-long data for January, April, July and October. Harmonic analysis is carried out and the variations in the major five astronomical constituents (M2, S2, K1, O1 and N2) are examined. The study shows monthly variation is least in the case of the diurnal constituents, i.e., K1 and O1. On the contrary, seasonal variability is noticeable in the case of the semi-diurnal constituents. The maximum amplitude of 3.418 m is recorded for M2 in April. But

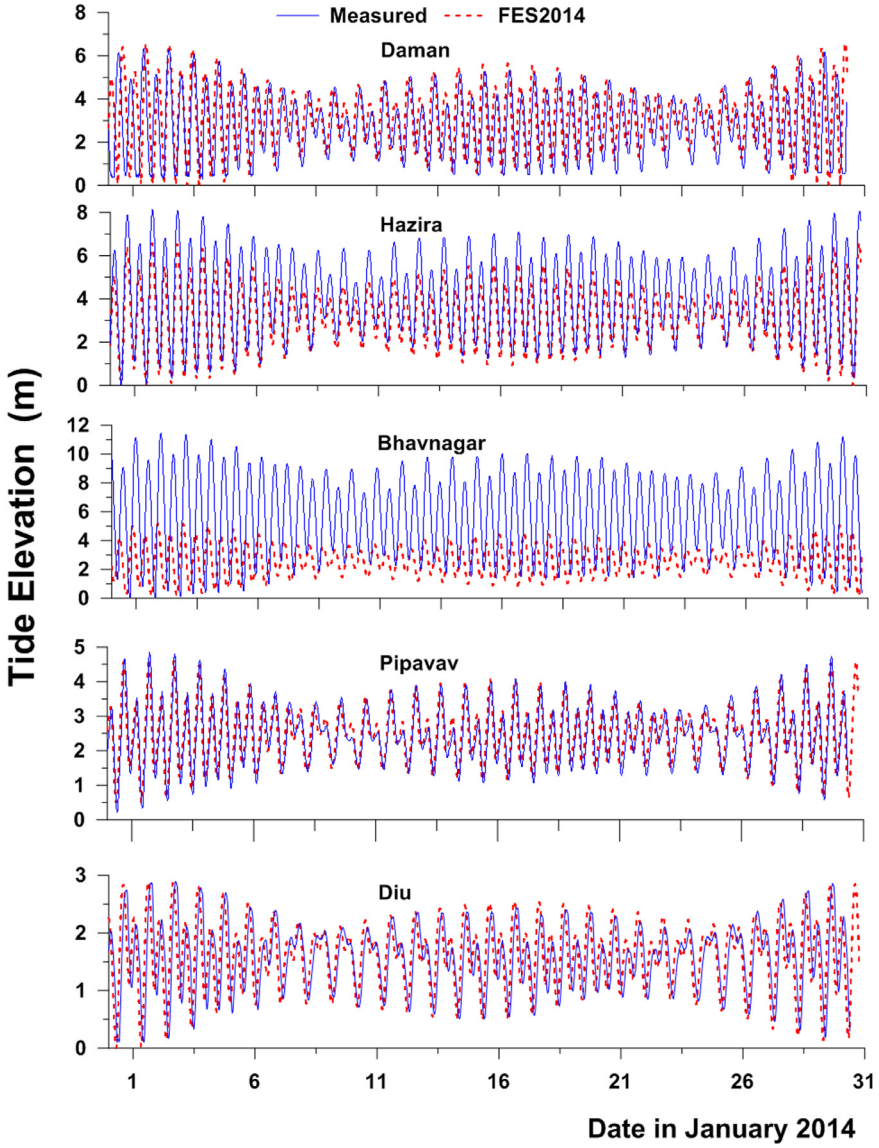

Figure 4 Comparison of FES2014 tide with the measured tide at Daman, Hazira, Bhavnagar, Pipavav and Diu.

Table 4 Comparison between major tidal constituents extracted from global model FES2014 and measured data.

Locations	M2 (m)		S2 (m)		K1 (m)		O1 (m)	
	FES2014	Measured	FES2014	Measured	FES2014	Measured	FES2014	Measured
Daman	1.65	1.72	0.74	0.64	0.55	0.54	0.22	0.24
Hazira	1.55	2.16	0.67	0.76	0.51	0.61	0.20	0.26
Bhavnagar	1.23	3.34	0.51	1.06	0.34	0.69	0.14	0.29
Pipavav	0.83	0.87	0.35	0.34	0.46	0.51	0.20	0.21
Diu	0.55	0.48	0.23	0.21	0.41	0.42	0.19	0.19

on an average, the maximum amplitude is recorded in July when the south-west monsoon is at its peak. The trend of propagation of diurnal and semi-diurnal constituents is similar, i.e., to increase from southern GoK towards the inner Gulf, reaching maxima in Bhavnagar, for every month. Still, the amplification of semi-diurnal tides is substantially high. Among the diurnal tides, the seasonal variability is prominent in the case of K1. O1 is found to be persistent for different seasons. In a nutshell, it could be noticed that the summer amplitudes are higher than the winter amplitudes and the open ocean stations have shown the least seasonal variability. The variability surmises the fact that the semi-

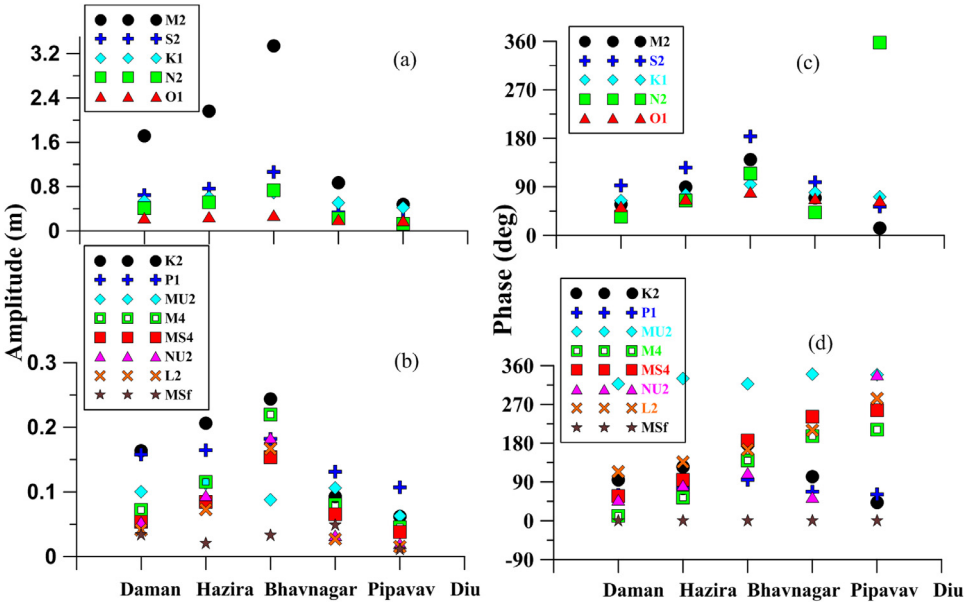

Figure 5 a) and b) Amplitude distribution of major astronomical tidal constituents at 5 locations in the study area based on measured data and the corresponding phase lag distribution is shown in c) and d).

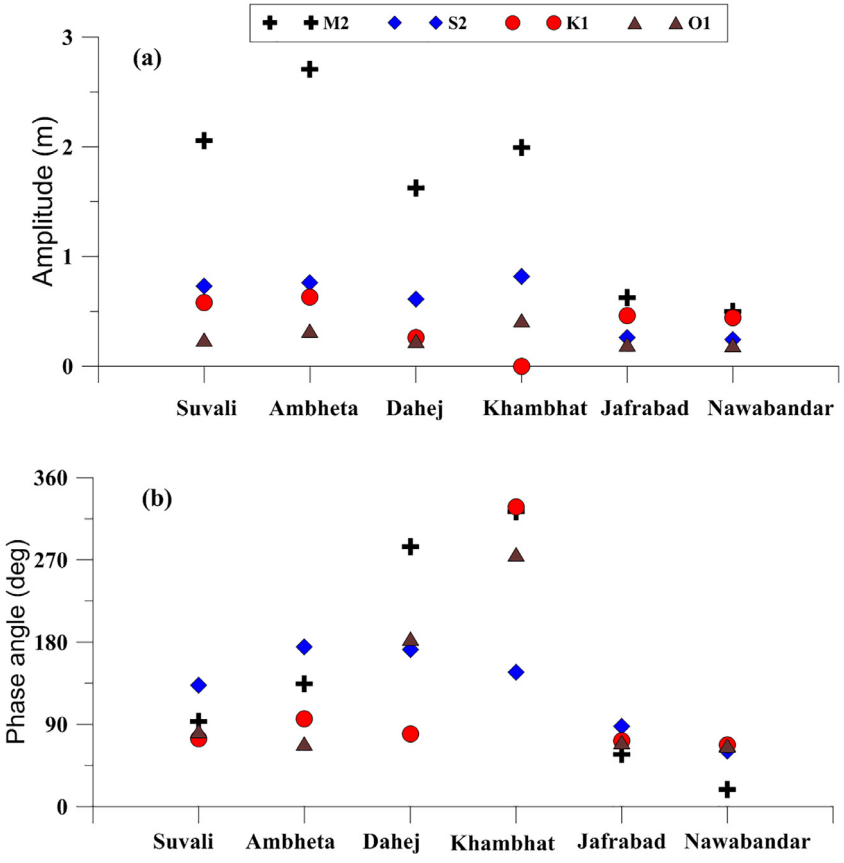

Figure 6 Amplitude and phase lag distribution of major astronomical constituents of MIKE21 Global Tide Model-derived tides in the study area.

diurnal constituents have spatial as well as temporal variation, while in the case of diurnal constituents, only the spatial variability is prominent.

4.3.2. Phase lag

Uniformity in the phase-changes for the selected locations has been obtained for all the major constituents except N2 and NU2; in these cases, a gradual increase in phase from Daman to Bhavnagar is noticed in case of eastern coast (Fig. 5c and d), but the phase got dramatically decreased from Diu to Pipavav which again increased in Bhavnagar. For all other cases, a gradual increase is observed from south to north along both the coasts. Similar trends of variation are noticed for K2 and P1. In the case of M4, MS4 and L2, a gradual increase in phase lag is obtained from Daman to Diu. There is no regular pattern of variation in the case of MU2.

A similar trend is followed in the case of MIKE21 Global Tide Model-derived data (Fig. 6b). M2 phase lag had an increase from Suvali (on the eastern coast) and Nawabandar (on the western coast) towards the north and reached the maximum at Khambhat. No other major constituents followed the same trend. The maximum phase lag is obtained in the northern-most location in the case of the diurnal constituents.

4.3.3. Spatial pattern of amplitudes and phase lags of major tidal constituents

Tide amplitudes derived at several places of the Gulf are used to determine the major tidal constituents. The MIKE21-Global Tide Model-simulated amplitudes resemble that of the observed. The spatial patterns of the amplitude of major constituents (K1, O1, M2 and S2) are presented in Fig. 7 and those of the phase lags are presented in Fig. 8. The contour lines of M2 suggest that the propagation of M2 is along the channel. The trend of propagation is similar in the case of S2, even though the amplitude of S2 is much lesser. Cross-channel propagation has been noticed in the case of the diurnal constituents (O1 and K1). Amplification of tides could easily be noticed from offshore towards the Gulf, but it is quite slower for the diurnal tide than the semi-diurnal. Gradual decreases in the phase lag are obtained from outer GoK to inner GoK for all other tidal constituents, except O1, where higher phase lag values are obtained inside the Gulf (Fig. 8).

4.3.4. Tidal form factor/tidal anomaly correlation

Tidal form factor (F) or tidal anomaly correlation, which is the ratio of the sums of the amplitudes of the two main diurnal constituents (K1 and O1) to that of the semi-diurnal constituents (M2 and S2) is estimated and presented in Table 5. The tide of a particular area could be classified according to the magnitude of the tidal form factor as; semi-diurnal ($0 < F < 0.25$), mixed and mainly semi-diurnal ($0.25 < F < 1.5$), mixed and mainly diurnal ($1.5 < F < 3.0$) and diurnal ($F > 3.0$).

There is a gradual decrease in the tidal form factor from Gulf mouth to head in the eastern and western GoK. The minimum magnitude is obtained at Bhavnagar (0.22), which gradually increased at Pipavav with a maximum at Diu on the western coast. The tidal form factor is found to increase from north to south, unlike the major tidal constituents, which increase from south to north. In addition to the mentioned locations, eight more locations are chosen throughout the Gulf, where the tidal form factor is calculated with the help of simulated tidal elevation (MIKE21 Global Tide Model-derived data). The minimum magnitude of 0.15 is obtained in the case of Khambhat (northern GoK). The maximum magnitude of the tidal form factor of 0.85 is noticed at Nawabandar, which situates at the south-western GoK in the Saurashtra coast.

Table 5 Tidal form factor at different locations.

Location	Tidal form factor
Daman (Measured)	0.33
Suvali (Simulated)	0.29
Hazira (Measured)	0.30
Ambheta (Simulated)	0.27
Dahej (Simulated)	0.22
Khambhat (Simulated)	0.15
Bhavnagar (Measured)	0.22
Jafrabad (Simulated)	0.75
Nawabandar (Simulated)	0.85
Pipavav (Measured)	0.60
Diu (Measured)	0.88

4.4. Monthly variation in MSL and SLA

Intra-annual variability in MSL is determined for the entire year from the measured as well as simulated data and is presented in Table 6. It had a gradual increase from Daman to Bhavnagar and then gradually decreased from Bhavnagar to Diu. MSL variations are more evident inside the Gulf (Bhavnagar) rather than the offshore locations (Daman and Diu). The maximum variation in the MSL (~0.25 m) is obtained in Bhavnagar. Although small variation in MSL is obtained for the entire year, maximum MSL is recorded during the south-west monsoonal months, which is associated with the monsoonal winds.

Monthly variation in SLA is observed for the entire year for each of the locations. The SLA-variability is found to be very less. Maximum SLA is observed during the monsoonal months in most of the stations, while minimum SLA is observed during pre-monsoon (Table 7).

4.5. Sea-level residual

The sea-level residual is extracted for a year at each location to obtain the inter-annual variability. The maximum residual sea-level is observed in Bhavnagar with a magnitude of around 0.7 m. Minimum tide residue of 0.17 m is obtained in Diu (Fig. 9). Even though there is a difference in the magnitude of the tidal residual, the trend of variation is similar at each location.

Wind data forJanuary 2014 is obtained and the correlation between the v-component of wind (alongshore wind) and the residual sea-level is estimated. A rise in sea-level could be noticed with an increase in the alongshore wind (Fig. 10). Even though a positive correlation between sea-level and v-component of wind is obtained for all the lo-

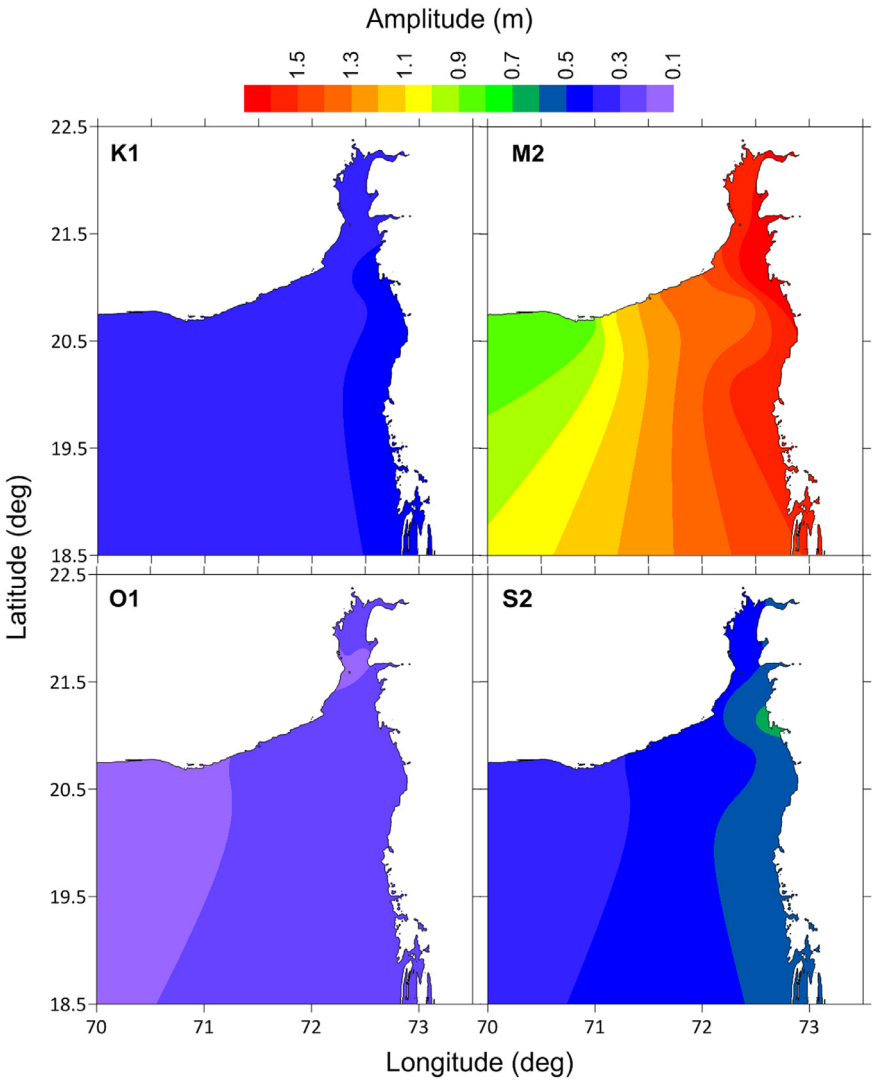

Figure 7 Contours of amplitudes of major tidal constituents (K1, M2, O1 and S2) of Gulf of Khambhat and surroundings.

Table 6 Monthly mean sea level (m) at different locations in different months.

Month	Daman	Suvali	Hazira	Ambheta	Dahej	Khambhat	Bhavnagar	Pipavav	Jafrabad	Nawabandar	Diu
Jan	2.87	3.60	4.1	4.22	4.88	4.12	5.74	2.47	1.85	1.37	1.49
Feb	2.92	3.60	4.15	4.20	4.92	4.13	5.80	2.49	1.85	1.37	1.51
Mar	2.97	3.61	4.19	4.23	4.88	4.13	5.89	2.46	1.85	1.38	1.53
Apr	2.93	3.60	4.16	4.23	4.89	4.13	5.85	2.38	1.86	1.38	1.48
May	2.95	3.60	4.19	4.23	4.89	4.13	5.87	2.37	1.86	1.39	1.47
Jun	2.90	3.60	4.32	4.22	4.90	4.13	5.99	2.50	1.85	1.38	1.70
Jul	3.03	3.60	4.23	4.22	4.91	4.13	5.84	2.47	1.85	1.37	1.70
Aug	3.03	3.60	4.23	4.21	4.92	4.13	5.83	2.47	1.84	1.35	1.70
Sep	2.97	3.60	4.16	4.21	4.91	4.13	5.85	2.47	1.84	1.37	1.70
Oct	2.93	3.60	4.17	4.20	4.92	4.13	5.76	2.47	1.84	1.35	1.71
Nov	2.95	3.60	4.24	4.21	4.90	4.13	5.85	2.47	1.85	1.37	1.70
Dec	2.88	3.59	4.15	4.21	4.90	4.13	5.72	2.46	1.85	1.37	1.70

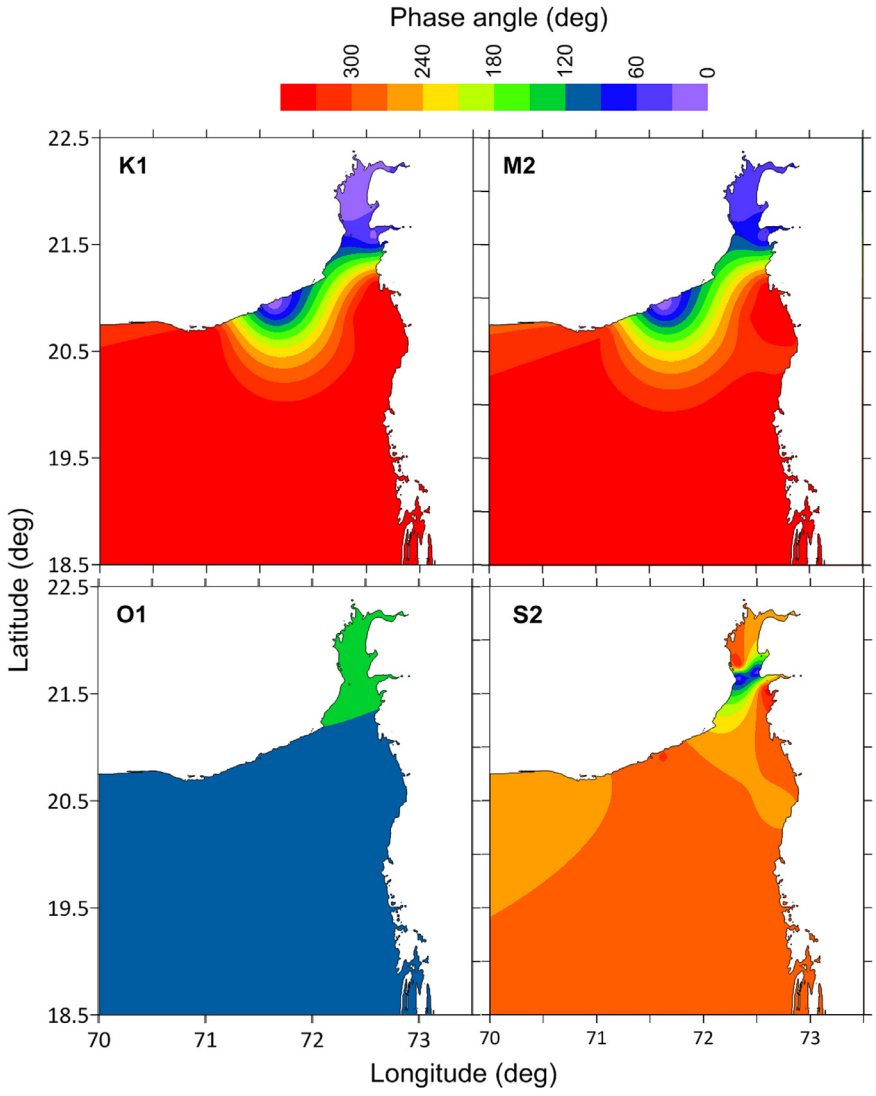

Figure 8 Contours of phase lags of major tidal constituents (K1, M2, O1 and S2) of Gulf of Khambhat and surroundings.

Table 7 Intra-annual variability of Sea Level Anomaly (SLA).

Month	Daman	Suvali	Hazira	Ambheta	Dahej	Khambhat	Bhavnagar	Pipavav	Jafrabad	Nawabandar	Diu
Jan	-0.07	0	-0.09	0	-0.02	-0.01	-0.09	0.01	0	0	-0.13
Feb	-0.02	0	-0.04	-0.02	0.02	0	-0.03	0.03	0	0	-0.11
Mar	0.03	0.01	0	0.01	-0.02	0	0.06	0	0	0.01	-0.09
Apr	-0.01	0	-0.03	0.01	-0.01	0	0.02	-0.08	0.01	0.01	-0.14
May	0.01	0	0	0.01	-0.01	0	0.04	-0.09	0.01	0.02	-0.15
Jun	-0.04	0	0.13	0	0	0	0.16	0.04	0	0.01	0.08
Jul	0.09	0	0.04	0	0.01	0	0.01	0.01	0	0	0.08
Aug	0.09	0	0.04	-0.01	0.02	0	0	0.01	-0.01	-0.02	0.08
Sep	0.03	0	-0.03	-0.01	0.01	0	0.02	0.01	-0.01	0	0.08
Oct	-0.01	0	-0.02	-0.02	0.02	0	-0.07	0.01	-0.01	-0.02	0.09
Nov	0.01	0	0.05	-0.01	0	0	0.02	0.01	0	0	0.08
Dec	-0.06	-0.01	-0.04	-0.01	0	0	-0.11	0	0	0	0.08

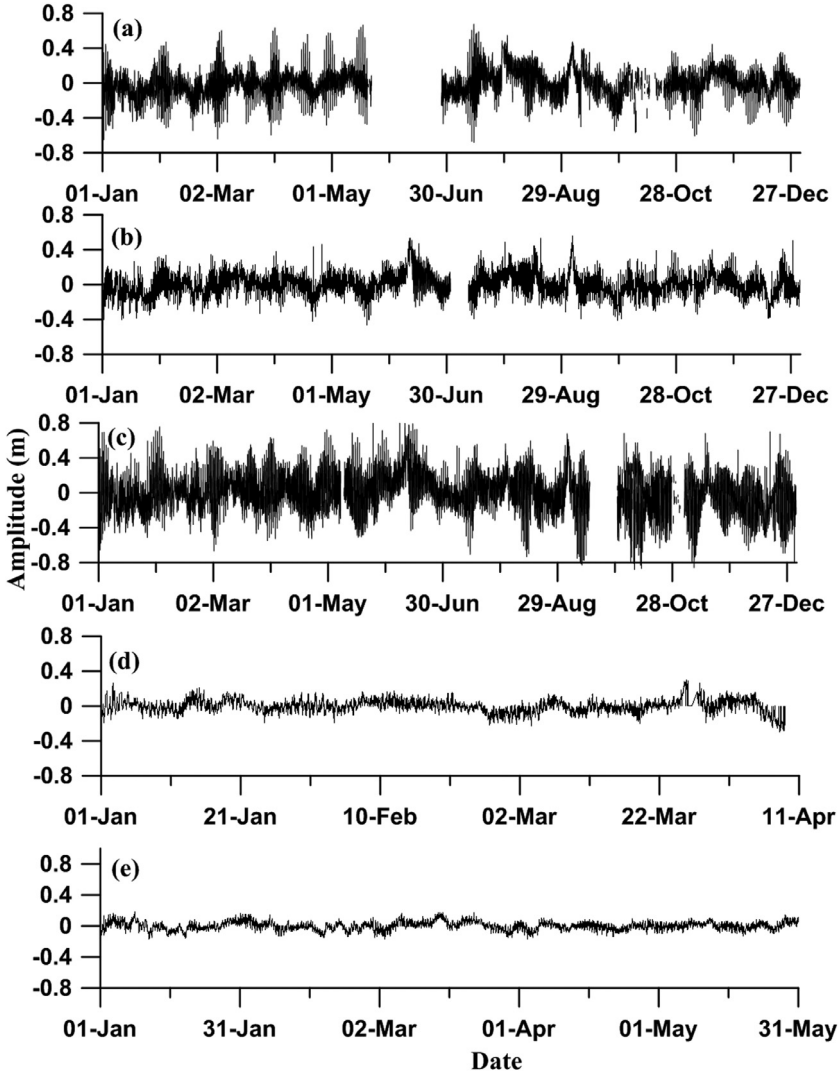

Figure 9 The non-tidal residual of sea-level at selected locations; a) Daman, b) Hazira, c) Bhavnagar, d) Pipapvav and e) Diu.

cations (Table 3), the significance level is very low for the inner Gulf locations. The maximum correlation has been noticed in the offshore stations (Daman and Diu). The seasonal wind regime of the area is portrayed in Fig. 10 for three typical months of pre-monsoon (March), southwest-monsoon (July) and northeast-monsoon (November), respectively. Maximum wind speed could be noticed inJuly, which is known as the peak monsoonal month. Wind speed reaches its maxima at the offshore locations irrespective of the seasons. Minimum wind impact could be observed inside the Gulf during March, but for other seasons, the magnitude of wind speed is considerable inside GoK.

5. Discussion

The measured and simulated tide elevation data indicates that it has a northward increase, reaches the maximum at the inner Gulf and had a slight decrease at the northernmost location. Tidal amplitude varies inside the Gulf at different rates; it is minimum for the southern stations and attains maximum inside the channel. The extremely variable channel geometry could explain these phenomena over a tidal cycle because, in a converging channel, the geometric effects amplify the incident wave and the rate of convergence depends on the channel convergence. Non-linearity in the tides could be illustrated by comparing the elevation of the Gulf-mouth (Pipavav) with that inside the Gulf (Hazira and Bhavnagar). The tidal amplification inside the Gulf resulted from the quarter wavelength resonance of the tides owing to its inherent geometrical settings (Nayak and Shetye, 2003). A similar condition was observed in the Gulf of Kachchh, west coast of India, where amplification of tidal amplitude arouse due to the convergence of the channel (Shetye, 1999). But the amplification of tides in the Gulf of Kachchh is quite smaller than that of GoK.

Tidal constituents followed a similar trend of variation as the tide elevation, which is quite evident. The amplitude maxima are found in the case of M2, which indicates the semi-diurnal dominance in the tide. The maximum M2 amplitude at Bhavnagar shows the amplification of M2 tide inside the Gulf. Amplification of semi-diurnal tide inside the Gulf is higher than that of the diurnal, which is in favour of the earlier studies. Semi-diurnal tides forced with neap

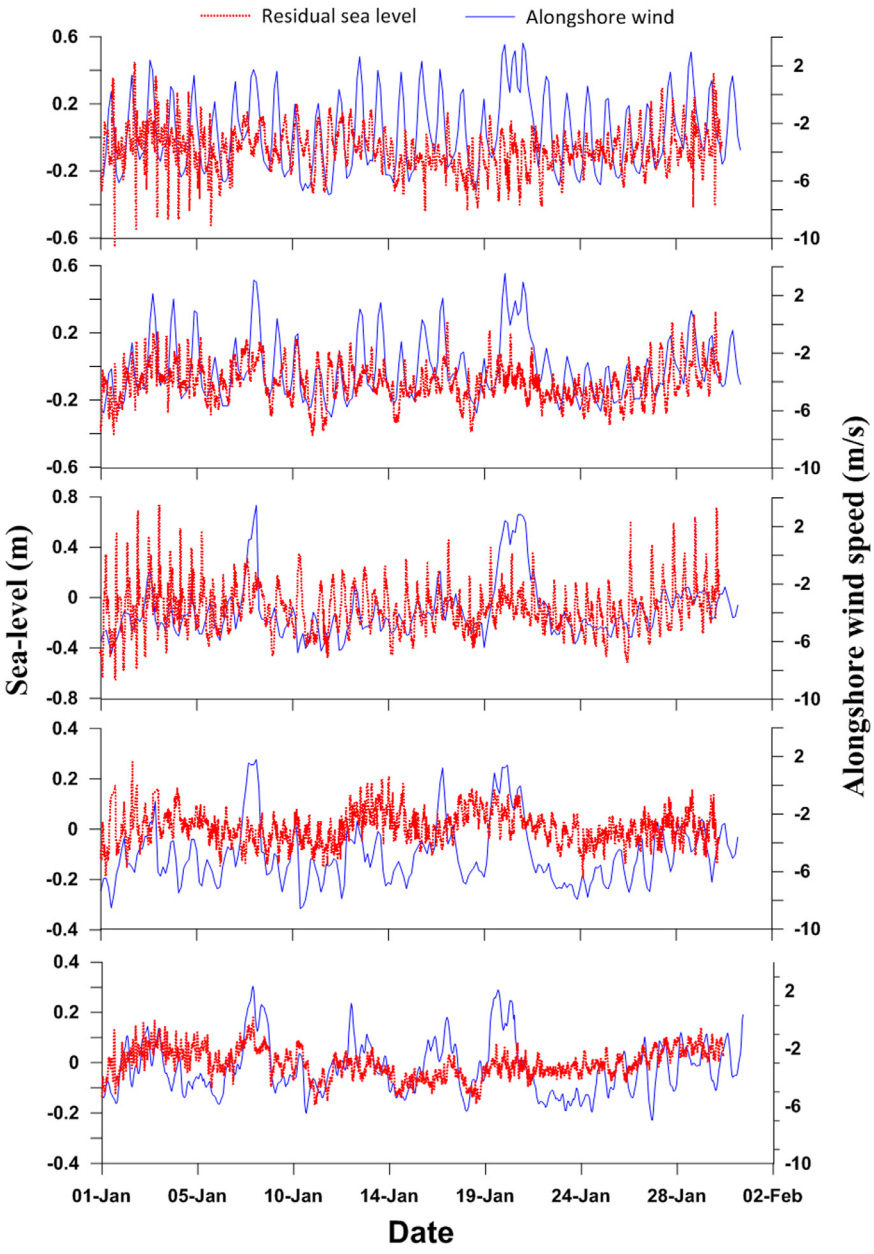

Figure 10 Comparison between the non-tidal residual of sea-level with the alongshore component of wind in January 2014.

and spring amplitudes at the estuary mouth exhibit similar properties along the upper reach, which is produced by the combined effect of reflection (that reduces friction) and enhanced morphological convergence in case of an ideal estuary (Garel and Cai, 2018); but in GoK, diurnal tides had amplification from mouth to head as resonance, together with geometric effects and friction, built up the amplification. Similar results were obtained from the study carried out by Nayak et al. (2015), where they obtained M2 amplitude of 0.40 m at the Gulf mouth, which has increased to 1.50 m inside the Gulf and decreased to 0.70 m at the Gulf head. A similar trend is followed by the other major constituents (S2, K1 and O1). The present study resembles the earlier work and reveals that amplitudes of the major tidal constituents have an increase from Daman (Gulf mouth) towards the inner Gulf and reached maxima in Bhavnagar, but had a further decrease in Khambhat (Gulf head).

The study also manifests the fact that the amplification is much higher on the western coast of the Gulf than on the eastern coast. The principal over-tide and compound tides are M4 and MU2, respectively. The trend of propagation of M4 (increasing from mouth to head) confirms the non-linearity of the system. If non-linearity is absent, the magnitudes of M4 would rapidly decrease within the channel from its small offshore values (Aubrey, 1985). M4 trend is also important for water and sediment transport purposes, which would be focussed on future research. By examining the neap/spring cycles at five stations within a month, it could be inferred that the non-linear distortion of the tide varies considerably. It is observed from the seasonal analysis that the average maximum amplitude is observed during

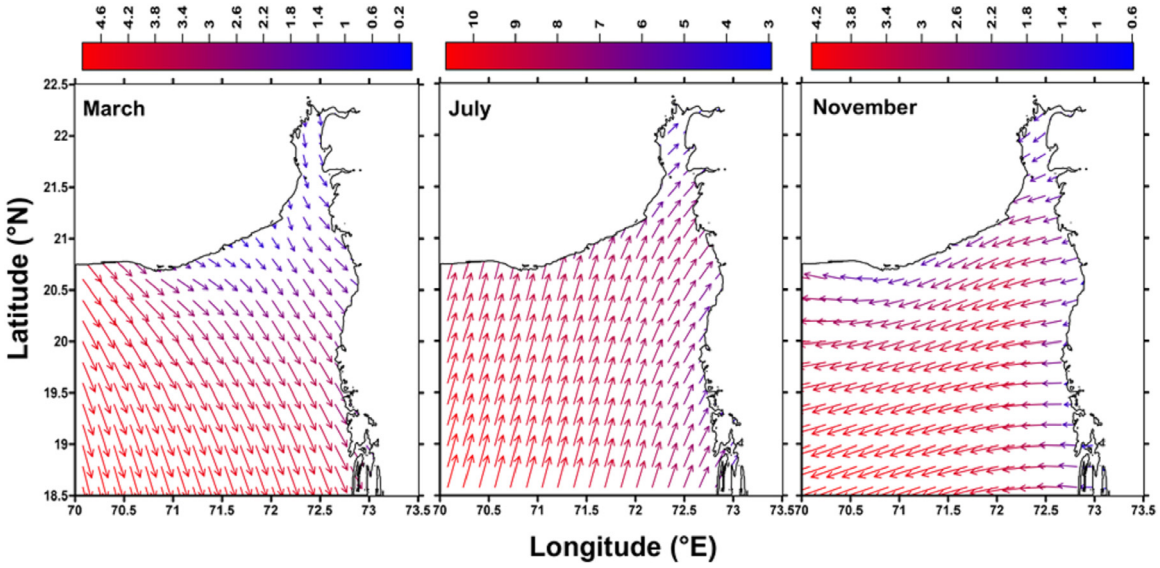

Figure 11 Seasonal wind regime of Gulf of Khambhat in March (representing pre-monsoon), July (representing monsoon) and November (representing post-monsoon).

July, which is due to the influence of peak south-west monsoon.

It should be noted that the tidal amplitude is greater during the flood flow rather than the ebb, which might accumulate sediment inside the GoK, which is known to be one of the major turbid water body of the west coast of India. Fine suspended sediment transport will be affected by the non-linear tidal distortion as well. Depending on the channel geometry, this effect becomes pronounced further in the Gulf, where the tide is more non-linear. Tidal non-linearity has implications for mass flux calculations commonly attempted in shallow water Gulf or estuaries. The numerical simulations of Lee et al. (2016) in Delaware Bay and the Chesapeake Bay concluded that the shape of estuaries and bays could also affect the tidal amplitude. Thus it could be inferred that the funnel shape of the Gulf also enhances the tidal amplification along with the other factors. The quarter diurnal compound tides include the major constituent MS4, derived from the interaction of M2 and S2, which lags the forcing tides (M2+S2). This phase relationship also enhances the tide asymmetry favouring flood. The consistency of the phase lead/lag in all over-tides and compound tides throughout the Gulf suggest it is a property of a Gulf as a whole and not just of local characteristics. If the compound tide amplitudes are much smaller than the forcing constituents, they are insignificant to the tidal energy balance. The growth of MSf inside the Gulf is not consistent; rather, its amplitude depends upon atmospheric conditions, suggesting it is not a simple compound tide. Higher value in MSf amplitude indicates atmospheric disturbances such as storms.

Tide-prediction with monthly-, semi-annually- and annually-averaged datasets has shown that the more the number of data, the less error it would be in the predicted tide. Even though the monthly analysis data could predict the tide amplitude quite accurately, the best fit is found in the case of the yearly analysis data. The contour lines of diurnal and semi-diurnal constituents are found to be along channel and cross-channel respectively inside the Gulf and the amplification of M2 tide is much higher than that of the others. The inherent geometry of the Gulf is responsible for these orientations (Nayak et al., 2015). Gradual changes in phase lag from outer to inner GoK indicate the propagation of tide inside the channel.

The magnitude of the tidal form factor is found to be less in the eastern GoK, indicating the dominance of the semi-diurnal tides. A higher value of tidal form factor is obtained in the offshore location both for the eastern and western GoK, which gradually decreased towards the inner Gulf reaching its minima at the northern-most location, Khambhat. Thus it could be inferred that the semi-diurnal components mainly contribute to the tidal amplification from southern GoK towards the north. In the western Gulf, a higher value of tidal form factor manifested comparatively better dominance of the diurnal tides. The tidal form factor calculated inside the Gulf revealed that in the eastern as well as northern GoK, the dependence of the diurnal tide on the semi-diurnal is very less. But at the south-western GoK, it is more and reaches the maximum outside the Gulf on the western coast. The values are nearly equal to 1 in Diu and Nawabandar, which indicate that even a small change in semi-diurnal tide would lead to a change in the diurnal tide vice-versa in those locations. Overall, based on the magnitudes of the tidal form factor, the tides of GoK are classified as mixed and predominantly semi-diurnal in nature. The sea-level data of the entire year shows that the astronomical tide is mainly responsible for the sea-level variation.

Tide prediction is carried out with the help of tidal constituents estimated from monthly, half-yearly and annual time series (Table 8). Tidal amplitudes are found to be 1 to 10% lower in case of the estimate based on monthly time series compared to the annual one. Tides are 1 to 6% lower in case of the estimate based on six-monthly time series compared to the annual one.

Very less variation in the MSL is observed throughout the year for each location, but an increase in MSL is recorded

Table 8 Predicted tide during spring and neap tide using tidal constituents estimated from monthly, half-yearly and annual measured time series data. The values in brackets show the percentage reduction from the longest time series.

Locations	1 month data		6 months data		1 year data	
	Neap	Spring	Neap	Spring	Neap	Spring
Daman	5.23 (5.4%)	5.95 (1.2%)	5.43 (1.8%)	6.02 (2.0%)	5.53	6.14
Hazira	7.12 (10.0%)	7.93 (2.5%)	7.45 (5.8%)	8.13 (2.2%)	7.91	8.31
Bhavnagar	10.26 (3.1%)	10.96 (1.3%)	10.44 (1.4%)	11.11 (5.9%)	10.59	11.8
Pipavav	4.16 (1.9%)	4.59 (0.7%)	4.24	4.62	-	-
Diu	2.31 (1.7%)	2.55 (1.9%)	2.35	2.60	-	-

during the monsoonal months due to strong monsoonal winds. MSL could be affected by so many factors on a regional scale, but the major role is played by the overlying atmosphere. Changes in atmospheric pressure and wind stress are the primary cause of change in the MSL (Amiruddin et al., 2015; Wouters et al., 2011), which would eventually have an impact on the wind pattern of the area. Although the non-tidal sea-levels had smooth trends throughout the year, there are some discrete undulations, which could be the effect of the atmospheric disturbance (IMD report, 2014). The positive correlation between the tide residual and the v-component manifests the dependence of the non-tidal component of sea-level on the atmospheric processes, but the atmospheric influence gets diminished inside the Gulf. Estuarine water levels are influenced primarily by astronomical tides and coastal processes and secondarily by river flow (Jay et al., 2015). Even though the river discharge could have an influence on the MSL variability of Gulfs and estuaries, its effect is found to be negligible in GoK. The major discharge is contributed by river Narmada, but its influence is found to be a purely localized phenomenon; it did not contribute to the Gulf dynamics as a whole (Mitra et al., 2020). Also, these sea-level variations, triggered by storm winds, could disturb the tide, which has an astronomical origin. Along the east coast of India, seasonal sea-level changes from atmospheric pressure variations vary from about 0.03 m at Colombo to 0.13 m at Paradip (Shankar, 2000). The impact of atmospheric pressure is not considered in the present study since there was no large variation in the atmospheric pressure as there was no cyclone during the study period. During the present study, the v-component of wind had a positive correlation with the sea-level throughout the year. Thus, in a nutshell, it could be inferred that the non-tidal sea-level rise is due to the alongshore component of wind, especially in the offshore stations. The seasonal wind regime of the area is also in accordance with this. It could be noticed well that even though the global tidal model accurately predicts the tide elevation data for the offshore locations, it fails to predict the same for the shallow areas where regional models should better be used. The global model data are less reliable in coastal zones than in the open ocean because of inaccurate geophysical corrections and noisier radar impulse responses (Deng and Featherstone, 2006). The performance of the global models in shallow water and coastal zones is inferior to their performance in the open ocean in terms of the accuracy of tidal constituent estimations and, consequently, the accuracies of tidal height predictions (Ray et al., 2011). But it is worth mentioning that neither the physics-based nor the observation-based methods can provide the exact (error-free) tide predictions (Simkooei et al., 2014).

6. Conclusion

Sea-level data collected at five locations in the Gulf revealed that the astronomical tides are mainly responsible for the sea-level variation in this area. Tide propagates from Gulf mouth to head in a non-linear fashion. The major non-tidal factor contributing to the sea-level is the alongshore component of wind, which shows a positive correlation with the sea-level for each location. The amplitude of the major tidal constituents (M2, S2, O1 and K1) at Bhavnagar is 3.33, 1.06, 0.69 and 0.28 m and at Diu is 0.48, 0.21, 0.42 and 0.19 m respectively which infers the dominance of the semi-diurnal component in the tidal amplification. The summer amplitudes of the major tidal constituents are much higher than that of the winter amplitudes and the seasonal variability of the tidal constituents is comparatively higher in the inner stations than that of the offshore stations. The tidal form factor calculated for the locations in the Gulf indicates that tides in these areas are mixed and predominantly semi-diurnal in nature. The phase lag of MS4 tide from that of M2 and S2 exhibits the dominance of flood over ebb in this area, resulting to accumulation of sediment in the Gulf. Among the two models used in the present study, the global tide model FES2014 largely underestimates the tides inside the Gulf. In contrast, the MIKE21 Global Tide Model could predict the same more accurately.

Acknowledgements

The data used in the study is measured by the National Institute of Technology, Chennai. Director, CSIR-National Institute of Oceanography, Goa and Director, National Institute of Ocean Technology, Chennai, encouraged to carry out the study. We thank Dr. Udhaba Dora, Scientist, CSIR-NIO Regional Centre, Mumbai, for helping with the MIKE21 tide data. We thank both the reviewers and the Editor for the suggestions, which improved the scientific content of the paper. We thank all colleagues for the help provided during the field data collection. This is NIO contribution 6550 and forms a part of the Ph.D. thesis of the first author registered at Bharathidasan University, Tiruchirappalli, India.

References

Aubrey, D.G., Speer, P.E., 1985. A study of non-linear tidal propagation in shallow inlet/estuarine systems part I: observations. Estuar. Coast. Shelf Sci. 21, 185—205, https://doi.org/10.1016/0272-7714(85)90096-4.

Amiruddin, A.M., Haigh, I.D., Tsimplis, M.N., Calafat, F.M., Dangendorf, S., 2015. The seasonal cycle and variability of sea level in the South China Sea. J. Geophys. Res.-Oceans 120, 5490—5513, https://doi.org/10.1002/2015JC010923.

Bell, C., Vassie, J.M., Woodworth, P.L., 2000. POL/PSMSL Tidal Analysis Software Kit 2000 (TASK-2000). In: Permanent Service for Mean Sea Level, CCMS Proudman Oceanographic Laboratory, Bidston Observatory. Birkenhead, Merseyside, U.K., https://www.psmsl.org/train_and_info/software/task2k.php (accessed on 03/10/2018).

Carl, T.F., Aubrey, D.G., 1994. Tidal propagation in strongly convergent channels. J. Geophys. Res.-Oceans 99 (C2), 3321—3336, https://doi.org/10.1029/93JC03219.

Carrere, L., Lyard, F., Cancet, M., Guillot, A., 2015. FES 2014, a new tidal model on the global ocean with enhanced accuracy in shallow seas and in the Arctic region. In: In Proceedings of the EGU General Assembly 2015. Vienna, Austria, 12—17 April 2015.

Cartwright, D.E., Taylor, R.J., 1971. New computations of the tide-generating potential. Geophys. J. Int. 23, 45—73, https://doi.org/10.1111/j.1365-246X.1971.tb01803.x.

Deng, X., Featherstone, W.E., 2006. A coastal retracking system for satellite radar altimeter waveforms: Application to ERS-2 around Australia. J. Geophys. Res.-Oceans 111, https://doi.org/10.1029/2005JC003039.

Devlin, A.T., Jay, D.A., Talke, S.A., Zaron, E., 2014. Can tidal perturbations associated with sea level variations in the western Pacific Ocean be used to understand future effects of tidal evolution? Ocean Dynam. 64, 1093—1120, https://doi.org/10.1007/s10236-014-0741-6.

Devlin, A.T., Jay, D.A., Zaron, E.D., Talke, S.A., Pan, J., Lin, H., 2017a. Tidal variability related to sea level variability in the Pacific Ocean. J. Geophys. Res.-Oceans 122, 8445—8463, https://doi.org/10.1002/2017JC013165.

Devlin, A.T., Jay, D.A., Talke, S.A., Zaron, E.D., Pan, J., Lin, H., 2017b. Coupling of sea level and tidal range changes, with implications for future water levels. Sci. Rep. 7, 17021, https://doi.org/10.1038/s41598-017-17056-z.

Devlin, A.T., Pan, J., Lin, H., 2019. Tidal variability in the Hong Kong region. Ocean Sci. 15, 853—864, https://doi.org/10.5194/os-15-853-2019.

DHI, 2017. MIKE 21 Toolbox Global Tide Model — Tide Prediction, 116, https://www.dhigroup.com/download/mike-by-dhi-tools/coastandseatools/global-tide-model (accessed on 26.02.2019).

Dronkers, J.J., 1964. Tidal Computations in Rivers and Coastal Waters. North-Holland Publ. Comp., Amsterdam, 516 pp., https://doi.org/10.1126/science.146.3642.390 .

Garel, E., Cai, H., 2018. Effects of Tidal-Forcing Variations on Tidal Properties Along a Narrow Convergent Estuary. Estuar. Coasts 41, 1924—1942, https://doi.org/10.1007/s12237-018-0410-y.

Godin, G., 1993. On tidal resonance. Cont. Shelf Res. 13 (1), 89—107, https://doi.org/10.1016/0278-4343(93)90037-X.

Jay, D.A., Leffler, K., Diefenderfer, H.L., Borde, A.B., 2015. Tidal-Fluvial and Estuarine Processes in the Lower Columbia River: I. Along-Channel Water Level Variations. Pacific Ocean to Bonneville Dam. Estuar. Coasts 38, 415—433, https://doi.org/10.1007/s12237-014-9819-0.

Joseph, A., Vijaykumar, K., Mehra, P., Unnikrishnan, A.S., Sundar, D., Prabhudesai, R.G., 2009. Observed tides at Mumbai High offshore region near the continental shelf break in the eastern Arabian Sea. Current Sci. 96 (9), 1233—1235.

Kalnay, E., Kanamitsu, M., Kistler, R., Collins, W., Deaven, D., Gandin, L., Iredell, M., Saha, S., White, G., Woollen, J., Zhu, Y., Leetmaa, A., Reynolds, R., Chelliah, M., Ebisuzaki, W., Higgins, W., Janowiak, J., Mo, K.C., Ropelewski, C., Wang, J., Roy, J., Joseph, D., 1996. The NCEP/NCAR 40-year reanalysis project. Bull. Am. Meteorol. Soc. 77, 437—471, https://doi.org/10.1175/1520-0477(1996)077%3C0437:TNYRP%3E2.0.CO;2.

Kumar, V.S., Kumar, K.A., 2010. Waves and currents in tide dominated location off Dahej. Gulf of Khambhat. Mar. Geodesy 33, 218—231, https://doi.org/10.1080/01490419.2010.492299.

Kumar, V.S., Dora, G.U., Philip, S., Pednekar, P., Singh, J., 2011. Variations in tidal constituents along the nearshore waters of Karnataka, west coast of India. J. Coast. Res. 27 (5), 824—829, https://doi.org/10.2112/JCOASTRES-D-09-00114.1.

Kumar, V.S., Pathak, K.C., Pednekar, P., Raju, N.S.N., Gowthaman, R., 2006. Coastal processes along the Indian coastline. Current Sci. 91 (4), 530—536.

Lanzoni, S., Seminara, G., 1998. On tide propagation in convergent estuaries. J. Geophys. Res.-Oceans 103 (C13), 30793—30812, https://doi.org/10.1029/1998JC900015.

Lee, S.B., Li, M., Zhang, F., 2016. The effect of sea level rise on Tidal Dynamics in Chesapeake and Delaware Bays. In: Ocean Sciences Meeting 2016. EC31A-06, 1—26 February, New Orleans, Louisiana, USA., https://agu.confex.com/agu/os16/preliminaryview.cgi/Paper93354.html.

Liu, J.T., Aubrey, D.G., 1993. Tidal residual currents and sediment transport through multiple tidal inlets. Coast. Estuar. Stud. 44, 113—157, https://doi.org/10.1029/CE044p0113.

Mitra, A., Kumar, V.S., Naidu, V.S. , 2020. Circulation in the Gulf of Khambhat- A Lagrangian Perspective. J. Mar. Sci. Eng, 8, 25 pp., https://doi.org/10.3390/jmse8010025.

Nayak, R.K., Shetye, S.R., 2003. Tides in the Gulf of Khambhat, west coast of India. Estuar. Coast. Shelf Sci. 57, 249—254, https://doi.org/10.1016/S0272-7714(02)00349-9.

Nayak, R.K., Salim, M., Mitra, D., Sridhar, P.N., Mohanty, P.C., Dadhwal, V.K., 2015. Tidal and Residual Circulation in the Gulf of Khambhat and its Surrounding on the West Coast of India. J. Indian Soc. Remote Sens. 43, 151—162, https://doi.org/10.1007/s12524-014-0387-3.

Pugh, D.T., 1987. Tides, Surges and Mean Sea Level. John Wiley and Sons, Chichester, U.K., 472 pp., http://eprints.soton.ac.uk/id/eprint/19157 .

Ray, R.D., Egbert, G.D., Erofeeva, S.Y., 2011. Tide Predictions in Shelf and Coastal Waters: Status and Prospects. In: Vignudelli, S., Kostianoy, A., Cipollini, P., Benveniste, J. (Eds.), Coastal Altimetry. Springer, Berlin, Heidelberg, 191—216.

Seifi, F., Deng, X., Andersen, O.B. , 2019. Assessment of the Accuracy of Recent Empirical and Assimilated Tidal Models for the Great Barrier Reef, Australia. Using Satellite and Coastal Data. Remote Sens, 11, 1211 pp., https://doi.org/10.3390/rs11101211.

Shankar, D., 2000. Seasonal cycle of sea level and currents along the coast of India. Current Sci 78 (3), 279—288.

Shetye, S.R., Gouveia, A.D., 1998. Coastal circulation in the North Indian Ocean — Coastal Segment (14, S—W). The Sea, 11. John Wiley and Sons, Inc., 523—772.

Shetye, S.R., 1999. Tides in the Gulf of Kutch. Cont. Shelf Res. 19, 1771—1782, http://dx.doi.org/10.1016/S0278-4343(99)00038-2.

Simkooei, A.R.A., Zaminpardaz, S., Sharifi, M.A., 2014. Extracting tidal frequencies using multivariate harmonic analysis of sea level height time series. J. Geodesy 88, 975—988, https://doi.org/10.1007/s00190-014-0737-5.

Sundar, D., Shankar, D., Shetye, S.R., 2005. Sea level during storm surges as seen in tide-gauge records along the east coast of India. Current Sci. 22, 1—10, https://www.jstor.org/stable/24104426.

Unnikrishnan, A.S., Shetye, S.R., Michael, G.S., 1999. Proc. Indian Acad. Sci. (Earth Planet Sci.) 108, 155—177, https://doi.org/10.1007/BF02842329.

Wijeratne, E.M.S., Woodworth, P.L., Stepanov, V.N., 2008. The Seasonal Cycle of Sea Level in Sri Lanka and Southern India. Western Indian Ocean. J. Mar. Sci. 7 (1), 29—43, https://doi.org/10.4314/wiojms.v7i1.48252.

Woodworth, P.L., 2017. Differences between Mean Tide Level and Mean Sea Level. J. Geodesy 91, 69—90, https://doi.org/10.1007/s00190-016-0938-1.

Wouters, B., Riva, R.E.M., Lavallée, D.A., Bamber, J.L., 2011. Seasonal variations in sea level induced by continental water mass: First results from GRACE. Geophys. Res. Lett. 38, L03303, https://doi.org/10.1029/2010GL046128.